PHY324: Measuring the gyromagnetic ratio using the relation between the resonant absorption frequencies of an electron in a DPPH radical and the magnetic field generated by a current flowing through Hemholtz coils

By: Gurmanjot Singh and Aran Wade

Due: 7 March 2023

1 Abstract

In this report, we will use the modelled relation between the absorption of high frequency photons–by electrons transitioning between spin states in free radical sample DPPH–and the magnetic field induced by a current in Hemholtz coils surrounding the sample, to compute a value for the gyromagnetic ratio of the free electron $\gamma = 1.78 \times 10^{11} \pm 6.90 \times 10^{-3}$ C/kg and the Lande factor $g = 2.02 \pm 0.02$. By comparing these to the accepted values, we then verify the model of electron spin resonance. We will also identify shortcomings in the experiment that result in perceived worse fitting systematically, invoking the fact that the accepted constants are within $\pm 1\%$ range of agreement with our computed values. We will then extend the discussion to an interpretation of the physics behind qualitative observations in the experiment through the lens of this model.

2   Introduction and Theory

Quantum mechanics predicts that electrons have an intrinsic spin $\vec{S}$ which generates a magnetic dipole $\mu = \gamma \vec{S}$. In the presence of a magnetic field $\vec{B}$, this then produces a potential $E = -\vec{\mu}\vec{B} = -\gamma \vec{S} \cdot \vec{B}$ [1]. In the case where the magnetic field is purely in one direction, which we will label the $-z$ axis, we get that:

$$E = \gamma S_z B_z$$

When observed, we know that an electron's spin can collapse into one of two states: (i) $S_z = +\hbar/2$ and (ii) $S_z = -\hbar/2$. This gives us two energy levels on the potential that the electron can be in, $E = \pm \hbar \gamma B_z / 2$. A transition from the lower to higher energy state requires an external energy contribution of $\Delta E = \hbar \gamma B_z$.

If this contribution is given by a photon of frequency f, necessarily having $\Delta E = 2\pi \hbar f$, the frequency must be:

$$f = \frac{1}{2\pi} \gamma B_z$$

If our given free electron is subjected to a beam of light, only photons of this specific frequency will be absorbed. Note that this is in the case of an idealized free electron with a perfect magnetic field in the z direction.

In reality, the electron's potential is perturbed by various external effects that modify the potential over space and time–such as other electrons and the magnetic field not being perfectly uniform and time independent–which results in a range of absorption frequencies around this resonance.

Not only that, but the electron itself either will move due to the magnetic field–causing the field around it to vary–or is restricted to a certain bound orbit due to another local potential–such as being bound in a molecule's orbital. In practice, it is much more convenient to keep the electron in a bound orbit, as we can restrict its motion and thus precisely keep track of the frequencies it absorbs, which we will do in this experiment.

Particularly, we will consider a sample of unpaired electrons bound in the outermost orbital of the free radical diphenylpicryl hydrazyl (DPPH) and subject it to a magnetic field produced in the middle of two Hemholtz coils of radius R and number of turns $n = 320$ with an AC current I flowing through them. This field has a central magnitude given by:

$$B = \left(\frac{4}{5}\right)^{3/2} \frac{\mu_0 n I}{R}$$

which will approximately be the field that the electrons will experience if the Hemholtz coils are spaced by a distance equal to their radius, where $\mu_0 = 4\pi \times 10^{-7} \mathrm{N/A^2}$ is the permeability of free space. As this cannot be exact, this is an approximation that will lead to the smearing of the absorption of frequencies by the sample, since the magnetic field will be slightly different.

When we measure this absorption using the oscilloscope, we will see a resonant peak in the signal amplitude at a particular value for the current given a frequency of emission, corresponding to the value of the magnetic field at which the most absorption occurs. Since the model predicts the relation:

$$f = mI \quad , \quad m = \gamma \left(\frac{4}{5}\right)^{3/2} \frac{\mu_0 n}{2\pi R}$$

where , we can perform a fitting of this parameter and then produce a value for γ given by:

$$\gamma = \frac{5^{3/2}\pi m R}{4\mu_0 n}$$

A common approximation of γ is just $\gamma_0 = e/2M$–where e is the electron charge and M is its mass–which assumes the electron is a spherically symmetric uniform charge distribution. We can compare this to the one we compute using the Lande factor $g = \gamma/\gamma_0$, which is an important dimensionless constant describing the free electron's magnetic dipole in other fields of physics.

3   Procedure and Methods

For this experiment, a sample of inactive DPPH will be suspended in a container coil between two Hemholtz coils with a current flowing through them from a power supply in series, as shown in Figure 1. The middle coil will be connected to the ESR basic unit, which supplies a variable radio frequency (RF) field that that will generate the high frequency photons. There are three of these coil types, each with a different number of coils for a different range of frequencies (more turns, lower frequency range).
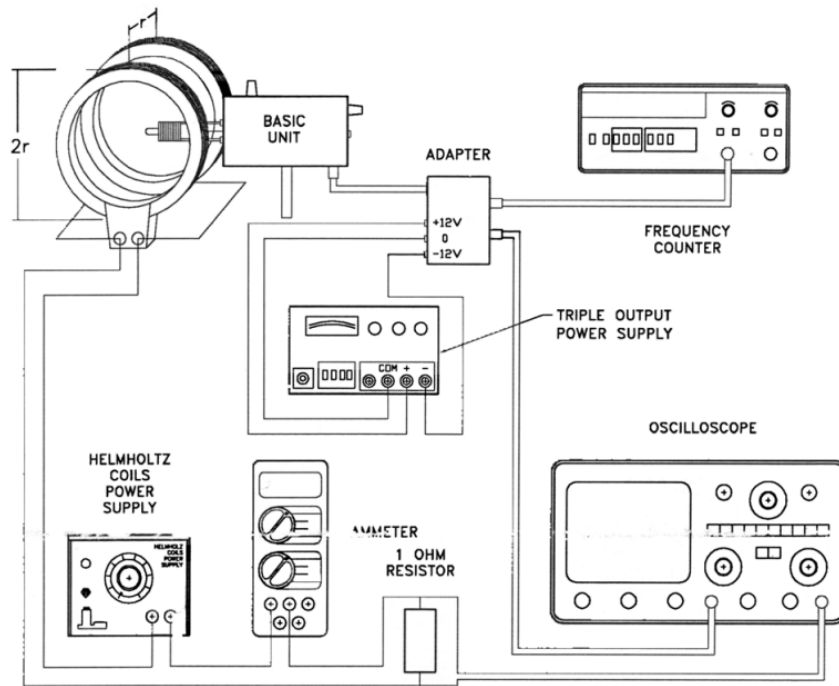

Figure 1: Electron spin resonance apparatus as described. See [2] for more details.

The frequency being provided is measured by a frequency counter connected to the ESR basic unit through the ESR adaptor, which is in turn connected to a power supply that is in series with a resistor and the Hemholtz coils. The resistor regulates the current flow from the power supply,

which will let us control the current by changing the power input. We measure the AC current using an ammeter placed in series. Note that this measures the effective DC current that would generate a power equivalent to that of the actual AC current, which in this case is twice the AC current magnitude [3]. This means the direct modulation current is half the measured values for current by the ammeter.

An oscilloscope is connected to the frequency counter and the ESR adaptor to measure the magnetic field absorption signal for the given frequency. This will resemble a periodic wave on the screen with two split peaks in each period. For a fixed frequency, when the current is varied, these peaks either move towards or away from each other. If we adjust so that they come closer, eventually there is a current at which the peaks merge and form a single large peak. The current at which this peak is the largest corresponds to the one generating the magnetic field that has the most frequency absorption–that is, our resonant frequency.

The frequencies we will be doing this for are of the 10^6 Hertz. Particularly, we will vary the frequencies from 19 MHz to around 80 MHz over all three coil types, with increments of around 1 to 2 MHz for each one. This gave us resonant currents ranging from 0.337 to 1.453 amperes.

All the resonances of the two larger coils stayed in the 1 A range of the current the equipment could handle. For the last coil, the maximal resonant currents occurred at much larger values, so we decided to only take three resonant values for it on the lower end of its frequency range to prevent any equipment damage from prolonged high currents.

We also noticed that as the frequency field increased, the noise in the oscilloscope signal was amplified and the actual resonant peaks also increased in amplitude. This made it harder to pinpoint when the peak merging occurred exactly, which contributed some uncertainty to the resonant current identification. The split peaks also became less and less symmetric, leading to an asymmetric merging that could've caused additional errors.

We found that the current would also start higher and then slowly drop down to a point of stability, so we made sure to wait for the current to stop changing and then measured it. A similar result was seen for the frequency counter, but it was much faster, so there was no other adjustment needed.

4   Constants and Uncertainties

We choose the uncertainties of our constants based on the standard uncertainty in their particular measurements. For the radius $R = 7.25$ cm of the Hemholtz coils, which we measured as half the diameter taken with a ruler, we assigned an uncertainty by using the smallest increment of precision on the ruler (± 0.1 cm) as the uncertainty of the diameter and then cutting it in half, giving us $\Delta R = \pm 0.05$ cm.

The number of turns was given by the experimental apparatus as $n = 320$, which clearly has no uncertainty in it as an integer precise to count. The accepted value for the permeability of free space $\mu_0 = 4\pi \times 10^{-7}$ N/A^2 has a relative standard uncertainty–as per [4]–of $\Delta\mu_0/\mu_0 = \pm 1.5 \times 10^{-10}$. Likewise, the accepted value for the electron mass $M = 9.1 \times 10^{-31}$ kg has a relative standard uncertainty of $\Delta M/M = \pm 3.0 \times 10^{-10}$ [5].

On the other hand, the charge $e = 1.6 \times 10^{-19}$ C is considered a fundemental constant and is exact [6].

During the measurements of I, we saw random noise fluctuations in the readings after stabilizing of up to ± 0.001 A, which we will then take as our standard current uncertainty without accounting for how we decided the resonant current. As we recall from the previous section, we found that the resonance identification was more difficult qualitatively. Particularly, the single peak was indistinguishable from the merging double peaks for about $\pm 3\%$ around the range of values the current was near. For smaller current values, this will contribute a very small additional uncertainty that is negligible in relation to the standard uncertainty. However, this adjustment will provide the sufficient correction to the larger current values to account for the peak detection problem.

A similar thing occurred in the measurement for the frequencies, although more directly. That is, the frequency measurements started with a standard precision error uncertainty due to noise of ± 0.001 MHz. However, as the values of frequency that were being used got larger, the noise fluctuations and so the standard uncertainty increased up to around ± 0.004 MHz. This corresponds to a relative percent uncertainty of approximately $\pm 0.004\%$ at all frequency ranges.

Together, these give us the error bars on the measurements of current and frequency. Note we divide those of current by 2 as the direct current measurement. Since the value for the slope m will be computed using the curve fitting method in Python's library Scipy, the standard fitting uncertainty designated by the standard deviation in m given by the computation will be assigned to it.

When finding the uncertainties of direct computations between uncertain quantities, we use the standard quadrature computation of uncertainty via square sums of relative standard deviations [8]. For example, when we are finding the uncertainty on $\gamma_0 = e/2M$, we compute its relative uncertainty as:

$$\Delta \gamma_0 / \gamma_0 = \sqrt{(\Delta e/e)^2 + (\Delta M/M)^2}$$

as the square root of the sum of the squares of the other quantities' relative uncertainties in the product. This generalizes to the calculation for quantities like γ, which–given the formula we found in the introduction–has a relative uncertainty:

$$\Delta \gamma / \gamma = \sqrt{(\Delta m/m)^2 + (\Delta R/R)^2 + (\Delta \mu_0/\mu_0)^2}$$

We do the same calculation for the Lande g factor to get that $\Delta g/g = \sqrt{(\Delta \gamma/\gamma)^2 + (\Delta \gamma_0/\gamma_0)^2}$. Using this standard uncertainty propagation, as well as our previously equipped values for uncertainty, we can proceed with the analysis of our results.

5   Results and Analysis

Recall that we fit the current-frequency data to a line given by $f = mI$. The data in our experiment, along with the fit, is shown in Figure 2. We get a fit value for the parameter as $m = 1.12 \times 10^8 \pm 8.49 \times 10^3$ Hz/A.

Qualitatively looking at the graph, the fit seems relatively good. However, note that the error bars in the frequency are very small–so small that they can barely be seen. Because of this, any small errors in the residual differences are amplified tremendously, which is seen especially for the last few values at the tail end of the set. These will contribute large amounts to the chi-squared

4

value, which is why $\chi^2/DOF = 3.62 \times 10^5$ for this model (where the degrees of freedom in this case is 27 due to 28 data points and 1 fitting parameter).
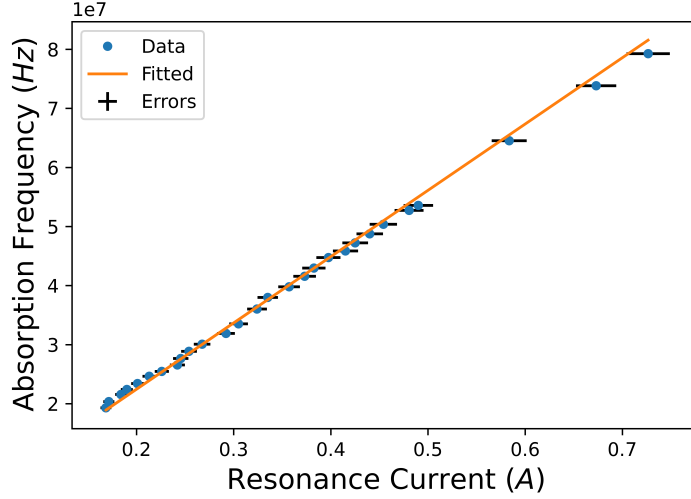

Figure 2: Absorption frequencies f (in Hz) plotted with the corresponding resonant currents I (in A), fitted by $f = mI$. The fitted value is $m = 1.12 \times 10^8$ Hz/A with uncertainty $\Delta m = 8.49 \times 10^3$ Hz/A. The reduced goodness of fit parameter is $\chi^2/DOF = 3.62 \times 10^5$.

The reason for this is also because the chi squared goodness of fit does not take into account uncertainties on the current axis, and so fails to take into account the fact that all the data points coincide with the line within the rectangle spanned by each points errorbars. Because of this, we have decided that chi-squared is not a very accurate depiction of how good the fit is.

Instead, we consider the residuals of the fit, given by the differences between the measured values of frequencies and the fitted values on the line. The error bars on these are computed by standard uncertainty propagation, taking the square root sum of the squares of the uncertainties and then square rooting them as follows [8]:

$$\Delta(\text{residuals}) = \sqrt{(\Delta f)^2 + (\Delta f_{\text{fit}})^2}$$

where the relative uncertainties on the fitted frequencies are just $\Delta f_{\text{fit}}/f_{\text{fit}} = \sqrt{(\Delta I/I)^2 + (\Delta m/m)^2}$ since $f_{\text{fit}} = mI$. This gives us a graph of residuals with widths, as shown in Figure 3. Between currents 0.15 A to 0.5 A, we see a relatively uniform spread of the residuals, which does not seem to show any particular trend. However, for the last three data points, we see a definitive downward trend that is not particularly indicative of anything given the error bars, but does suggest that the model might not be perfectly linear, especially for higher frequencies and currents.
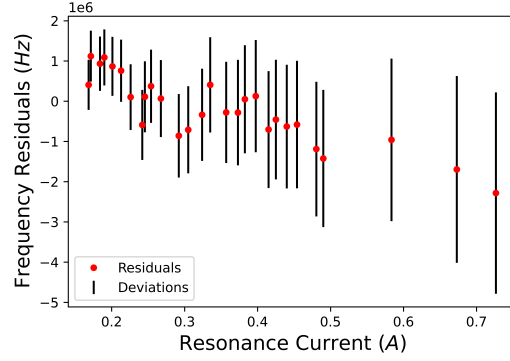
(a) Residuals with last three points.
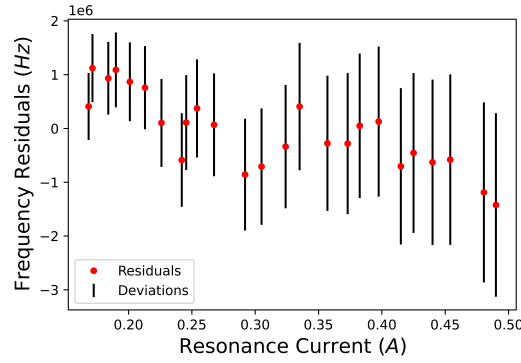
(b) Residuals without last three points.

Figure 3: Residuals of frequencies (Hz) plotted with the corresponding resonant currents and residual error bars. The trend looks like a very slow falling line to the right, but excluding the last three points makes this judgement much more difficult.

Since those last three currents correspond to the resonances that occurred beyond 1 A, it suggests that at and beyond the threshold, currents of the circuit might have a modified relation with the generated magnetic field of the coils. Conversely, it could be a result of consistently overestimating the current due to systematic error when looking for the peak, possibly from the additional identification imprecision at higher currents mentioned in the previous section. Since the increments were also much larger, and the window in which the measurement was concluded was smaller to avoid issues in the equipment, the chance for stabilization also was reduced, which would also cause this. This is encoded in the agreement of even these last three points within their rectangle of uncertainty with the fitted line.

It is unlikely that the ideal relation actually explicitly changes between the current and magnetic field other than how the current measurements were taken and possibly sort of fringe problem in the circuit due to the high currents. Although it is usually useful to plot the residuals in a histogram to check if they obey an approximate normal distribution to verify that they are independent, we do not have enough data to make a conclusion from this, as the bin count and range drastically change the shape. For reference, it looks as in Figure 4. We chose the number of bins to make sure the

6

distribution was connected and the overall shape of the distribution was captured. The error bars are given by the standard count uncertainty associated with histograms, as the respective square roots of the counts.
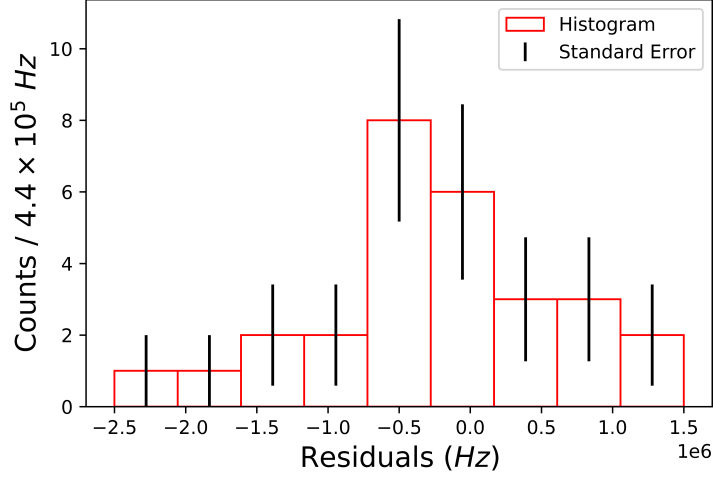

Figure 4: Histogram of frequency residuals, plotted with 9 bins in a range of $(-2.5 \times 10^6, 1.5 \times 10^6)$ Hz. This was decidedly the bin count and range that gave the most favourable shape after trial and error, but still is skewed to the right, suggesting that it is not Gaussian and has some dependencies in the residuals. We see that the mode of the histogram is not centered at 0 either, which suggests some consistent error in the fitting of the data points.

On that note, we compute our value for γ from the introduction–with uncertainty as outlined in the previous section–to be:
$$\gamma = 1.78 \times 10^{11} \pm 6.90 \times 10^{-3} \text{C/kg}$$

Using our propagation of uncertainty calculation and formula for γ_0, we also have that:

$$\gamma_0 = 8.79 \times 10^{10} \pm 6.24 \times 10^{-5} \text{C/kg}$$

So the value for the gyromagnetic ratio that our experiment predicts is around double the classical approximation. This comes up in our Lande g factor calculation, which up to sign contributed by the electron charge e is:
$$g = 2.02 \pm 0.02$$

According to the widely accepted value from NIST Reference on Constants, Units, and Uncertainty [7], the numerical value for g–when ignoring sign contributions–is $g_e = 2.002$, with a standard uncertainty of order 10^{-13}, which we can clearly neglect on the scale of our experiment.

Our value for g clearly coincides with g_e, and as the percentage error between the two is just $0.02/20 = 1\%$, they also agree statistically as they are within a 5% interval of each other, which means that there is high confidence in them agreeing and our experiment correspondingly having provided a meaningful value for g and γ.

7

This also validates our choice of model and again suggests that the fitting issues come from systematic errors and unaccounted for uncertainties within the analysis of the frequency errors.

6 Extensions

It is interesting to note that the experimentally determined gyromagnetic ratio and Lande g factor agree with that of the free electron, even though they were measured for a bound electron in the outer shell of a free radical in an imperfect magnetic field. This implies that the spin of an unpaired outer shell electron behaves very much like that of a free electron, which could find some use in other experiments relating to or involving electron spin.

This also hints at the phenomenon of paramagnetism in materials–induction of magnetic fields in a material as a response to external magnetic stimulus–given that the underlying model involves the same concept of the free electrons having two spin energy states that they can jump between.

We also decided that, if the apparatus were idealized, then the linear relation would never be broken, in the absence of systematic errors. However, this fails to acknowledge the possibility that the energy the electron absorbs could be used for another reason once a high enough frequency range is achieved: escape the atom and ionize it. Because of this, we would expect, even in the idealized case, for there to be a threshold frequency past which the sample starts emitting electrons, and so the absorption from the spin transition would decrease, resulting in less resonance. Note, however, that this would not change the absorption behaviour of the electron in the external magnetic field, just that some electrons would escape and possibly be unobservable in the formal lab setting.

Another important detail that does not particularly lie within the scope of this report is the width of the peaks in the ESR signal that we detect on the oscilloscope during the experiment. As the signal itself corresponds to magnetic field resonances of the sample of DPPH, the width is just the natural smeared uncertainty from a combination of hidden statistical and quantum effects on the resonant magnetic field value in the system. We mentioned previously that normally there would be two peaks for a fixed frequency and given current, which correspond to the two resonant values that the magnetic field oscillates through as the alternating current goes through one period, As these do not give maximum absorption, the conclusion is that when they merge to form the biggest peak does the full resonance occur.

Due to the uncertainty principle, this peak cannot be perfect and must have a width (or uncertainty) in the resonant magnetic field around the peak. This corresponds a factor proportional to the uncertainty in the transition energy δE, which by the uncertainty principle is related to the electron's spin decay time δt by $\delta E \delta t \approx \hbar$. Using the relationship between energy and the magnetic field, we get their uncertainties related by $\delta E = \hbar \gamma \delta B$ or that $\delta B \approx 1/(\gamma \delta t)$ as the width of the peak. Hence, the peak width is physically inversely proportional to the average time it takes for a spin-excited electron in the given magnetic field to decay back to its spin ground state, or essentially that the width is proportional to the rate of electron de-excitation. In theory, our previously computed values for γ and g could be used here to also determine this rate in the case of our system [3].

Also recall that the ESR signal was not perfectly symmetric, with the asymmetry becoming more pronounced as the frequency range increased. By this analysis, this implies that one of the split magnetic field resonances had more absorption than the other, which obviously would grow more

pronounced for higher frequencies as the peaks would also get larger. This would mean that the larger peak is asymmetrically closer to the actual resonance than the other peak, suggesting a sort of phase shift in the actual peaks so that they are not centered around the actual resonant magnetic field value. This means that, when they do merge, it might not be exactly at the peak, which gives another possible source of systematic error.

7   Conclusion

In the relationship between the current flowing through Hemholtz coils and the resulting resonant frequency of photons absorbed by a sample of electrons in the free radical DPPH due to spin transition, we were able to compute statistically and physically agreeable values for the gyromagnetic ratio $\gamma = 1.78 \times 10^{11} \pm 6.90 \times 10^{-3}$ C/kg and the Lande factor $g = 2.02 \pm 0.02$, with respect to the accepted value. In doing so, we verified the fitted model in the range of lower currents and frequencies, the data of which sufficiently agrees with the actual theory and would do so in a larger space of data if we had access to lab equipment with more precision and less room for systematic uncertainty.

In doing all this, we also developed a coherent interpretation for the physical meaning of components in the experiment's measurements, such as the width of the peaks in the ESR signal or the asymmetry of the split peaks. Altogether, this shows that the quantum effects of electron spin can have large scale physically observable effects, which makes this experiment a good starting point to consider other more complicated emergent quantum behaviour in physics.

References

[1] Ruxandra Serbanescu (2020), "Electron Spin Resonance." Last accessed on 7 March 2023 at `https://www.physics.utoronto.ca/~phy224_324/experiments/electron-spin-resonance/electric-spin.pdf`.

[2] Harrison (1988), "Electron Spin Resonance (with Leybold Instruction Sheet)." Last accessed on 7 March 2023 at `http://www.hep.fsu.edu/~wahl/phy4822/expinfo/esr/ESRutoronto.pdf`.

[3] *LD Physics Leaflets: Atomic and Nuclear Physics* (2012), "Electron spin resonance at DPPH." Last accessed on 7 March 2023 at `https://www.ld-didactic.de/documents/en-US/EXP/P/P6/P6262v1e.pdf`.

[4] *NIST Reference on Constants, Units and Uncertainty* (2019), "vacuum magnetic permeability." Last accessed on 7 March 2023 at `https://physics.nist.gov/cgi-bin/cuu/Value?mu0`.

[5] *NIST Reference on Constants, Units and Uncertainty* (2019), "electron mass." Last accessed on 7 March 2023 at `https://physics.nist.gov/cgi-bin/cuu/Value?me`.

[6] *NIST Reference on Constants, Units and Uncertainty* (2019), "elementary charge." Last accessed on 7 March 2023 at `https://physics.nist.gov/cgi-bin/cuu/Value?e`.

[7] *NIST Reference on Constants, Units and Uncertainty* (2019), "electron g factor." Last accessed on 7 March 2023 at `https://physics.nist.gov/cgi-bin/cuu/Value?gem|search_for=g+factor`.

[8] Vern Lindberg (2000), "Uncertainties and Error Propagation." Last accessed on 7 March 2023 at `https://www.geol.lsu.edu/jlorenzo/geophysics/uncertainties/Uncertaintiespart2.html`.